

# Performance Comparison of OFDM-TDMA and OFDMA with Cross-Layer Consideration

Yu-Jung Chang<sup>†</sup>, Feng-Tsun Chien<sup>‡</sup> and C.-C. Jay Kuo<sup>†</sup>

<sup>†</sup> Department of Electrical Engineering and Integrated Media Systems Center  
University of Southern California, Los Angeles, CA 90089-2564, USA

<sup>‡</sup> Department of Electronics Engineering, National Chiao Tung University, Hsinchu, Taiwan, ROC  
E-mails: yujungc@usc.edu, fchien@mail.nctu.edu.tw and cckuo@sipi.usc.edu

**Abstract**—Performance comparison of multiuser OFDM-TDMA and OFDMA systems by considering physical and link cross-layer behavior is conducted in this work. We provide a new framework for performance evaluation that centers on “scheduling” with several different subcarrier/bit allocation schemes. The performance metrics include: the bit rate, the bit error rate (BER), packet throughput and delay. The instantaneous channel conditions of users are assumed to be available at the base station, which can be achieved by channel estimation at the mobile terminal (MT), and then fed back to the base station through a control channel. To perform the link layer comparison, we model the Rayleigh fading channel with a finite-state Markov chain, and adopt the M/G/1 queueing model as the analytical tool. Computer simulation is performed to verify conducted analytical results.

## I. INTRODUCTION

In a multiaccess communication system where transmission resources are shared among multiple users, a resource management scheme is required. Time Division Multiple Access (TDMA) and Frequency Division Multiple Access (FDMA) are two well-known techniques for resource management based on the principle of time-sharing and frequency-sharing, respectively. When combined with OFDM (Orthogonal Frequency Division Multiplexing), they are called OFDM-TDMA and OFDMA (OFDM Access), respectively. Both of them have been adopted by the IEEE 802.16 standard as two options for transmissions at the 2–11 GHz band [1]. These two techniques have their pros and cons, and the main objective of this work is to compare them from the scheduling viewpoint with various subcarrier assignment and bit allocation schemes.

A way to share the resource in a multicarrier system is the allocation of subcarriers and bits among users across time and frequency domains. A dynamic subcarrier allocation strategy, where the allocation scheme depends on users’ instantaneous channel conditions, was shown to improve the system performance greatly (see, *e.g.*, [2]). Such a technique was adopted in [3] and [4] to provide performance comparison between OFDM-TDMA and OFDMA in terms of the bit error rate (BER). An uncoded result was shown in [4], where OFDMA with adaptive subcarrier/bit allocation outperformed OFDM-TDMA by 3 dB at BER =  $10^{-3}$ . A coded result was given in [3], where OFDMA with ideal subcarrier allocation (*i.e.*, the user with the highest signal-to-noise ratio (SNR) receives the subcarrier) was shown to outperform OFDM-TDMA by 7 dB.

The OFDM-TDMA scheme examined in [3] and [4] allocated predetermined time slots to users, where the allocation scheme is independent of user channel conditions. In other words, more effective OFDM-TDMA schemes such as channel-aware or opportunistically-scheduled OFDM-TDMA were not examined. Furthermore, little work has been done in the literature to compare OFDM-TDMA and OFDMA from a cross-layer viewpoint. We aim to address these issues in this work.

The link layer performance is interesting since multiuser resource

allocation is essentially a job of the medium access control (MAC) sublayer of the link layer. To perform the link layer comparison, we model the Rayleigh fading channel with a finite-state Markov chain, which is a technique widely used in previous studies, *e.g.*, [5]. Furthermore, the M/G/1 queueing model is used to provide a useful analytical tool. It is assumed throughout the work that instantaneous channel conditions of users are available at the base station. This can be achieved by channel estimation at the mobile terminal (MT), and then the estimated channel information is fed back to the base station through a control channel.

The rest of the paper is organized as follows. The basic framework of subcarrier assignment and bit allocation in the physical layer is described in Sec. II. The physical and link layer analysis for both OFDM-TDMA and OFDMA is presented in Sec. III. Simulation results are shown in Sec. IV. Finally, concluding remarks are given in Sec. V.

## II. SUBCARRIER ASSIGNMENT AND BIT ALLOCATION

In a multicarrier system, resource allocation in the physical layer is accomplished by subcarrier allocation and bit allocation. The system may (or may not) have the flexibility in assigning subcarriers to users depending on their channel conditions. Furthermore, if adaptive modulation is employed, the number of bits loaded to the assigned subcarrier can be determined dynamically. The basic idea of adaptive modulation is to employ high-order modulation schemes at subcarriers with high SNR, and vice versa. With adaptive modulation, the performance of an OFDM system can be greatly enhanced. Several different schemes will be described in this section based on their subcarrier assignment and bit allocation schemes.

### A. Subcarrier Assignment

TDMA and FDMA perform multiple access in a time-sharing and a frequency-sharing manner, respectively. OFDM-TDMA allocates OFDM symbols to users while OFDMA allocates subcarriers to users. Here, we consider a framed structure where each frame contains several OFDM symbols as shown in Fig. 1. The channel is assumed to be quasi-static in the sense that the channel condition varies across frames but remains the same within a frame. Under such a framed structure, we compare two OFDM-TDMA modes (static and dynamic) and one OFDMA mode (dynamic) as given in Table I. To the best of our knowledge, the study on dynamic OFDM-TDMA is new.

In static OFDM-TDMA, frames are allocated to users in a round-robin fashion, which is independent of their channel conditions. In dynamic OFDM-TDMA, each frame is allocated to a user with the best channel gain. In other words, the user is chosen to be

$$k' = \arg \max_k \sum_{l=0}^{L-1} |h_{k,l}|^2, \quad (1)$$

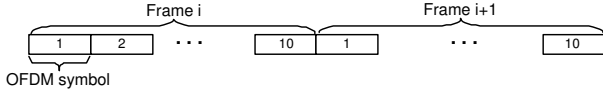


Fig. 1. Example of a frame that contains ten OFDM symbols.

TABLE I  
THREE MULTIACCESS OFDM MODES

Mode Name	Comments
OFDM I	static OFDM-TDMA
OFDM II	dynamic OFDM-TDMA
OFDMA	dynamic OFDMA

where  $h_{k,l}$  is the complex channel coefficient at the  $(l+1)$ th path of user  $k$ , and  $L$  is the number of paths. The best user is determined in the beginning of each frame. The approach is justified by the fact that the error probability decreases as the channel gain increases [6].

Note that the chosen user is allocated all subcarriers exclusively for all OFDM symbols within this frame in both OFDM-TDMA modes. In contrast, dynamic OFDMA allows multiple users to share subcarriers in an OFDM symbol. A subcarrier is allocated to the user with the best SNR seen at that particular subcarrier. The subcarrier assignment task is decided and performed in the beginning of each frame.

### B. Bit Allocation

For bit allocation, we adopt the discrete-rate adaptive modulation method [7]. That is, we first divide the received SNR value into several disjoint regions and determine their boundaries  $\bar{b} = \{b_0, b_1, b_2, b_3, b_4\}$  as shown in Fig. 2. Only square M-QAM modulations (4-, 16-, 64- and 256-QAM) are considered here. Both OFDM-TDMA and OFDMA determine the received SNR value for each region and select the proper modulation method accordingly. The set of boundaries  $\bar{b}$  can be determined as follows.

First, the BER expression for M-QAM is given by [7]:

$$P_b = 0.2 \exp\left(-\frac{3\beta}{2(M-1)}\right), \quad (2)$$

where  $\beta$  is the SNR value of the channel. Since  $M = 2^r$ , the required  $\beta$  value to send  $r$  bits at given  $P_b$  is equal to

$$\beta = -\frac{2}{3}(\ln 5P_b)(2^r - 1). \quad (3)$$

Second, by plugging  $r = \{0, 2, 4, 6, 8\}$  and the target BER  $P_b$  in (3), we obtain  $\bar{b}$  with  $b_0$  and  $b_5$  set to 0 and  $\infty$ , respectively. Thus,  $r$  bits are loaded when  $\beta \in \{b_{r/2}, b_{r/2+1}\}$ . Note that the resulting modulation scheme employed in each region guarantees a BER no higher than  $P_b$ .

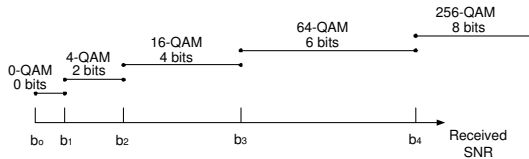


Fig. 2. Choice of adaptive modulation schemes as a function of the SNR value.

## III. ANALYTICAL PERFORMANCE COMPARISON

In this section, we analyze several performance measures for the three OFDM modes in Table I. These analytical results will be verified by simulation in Sec. IV.

### A. Bit Rate and BER Analysis

The theoretical bit rate upper bound will be derived under the assumption of the use of continuous-rate adaptation here. Since the discrete-rate adaptation always has a slower bit rate than the continuous-rate adaptation [7], the derived upper bound is also an upper bound for the discrete case, which is adopted in a practical environment.

For given  $P_b$  and  $\beta$ , we can obtain the bit rate per subcarrier from (2) as

$$r(\beta) = \lg M(\beta) = \lg\left(1 + \frac{1.5}{-\ln 5P_b}\beta\right), \quad (4)$$

where  $\lg$  is the base-2 logarithm. We will use  $\ln$  to denote the natural logarithm to differentiate these two logarithm functions. For a Rayleigh fading channel, the received SNR is an exponential random variable [5], denoted by  $\Gamma$ , with the following probability density function (pdf)

$$g(\gamma) = \frac{1}{\gamma_0} \exp\left(-\frac{\gamma}{\gamma_0}\right), \quad \gamma \geq 0, \quad (5)$$

where  $\gamma_0$  is the average SNR. The above analysis applies to both OFDM I and OFDM II except that they have a different mean. Due to dynamic selection, the mean of OFDM II is slightly higher, which will be confirmed by simulation results.

By averaging over the received SNR distribution, the bit rate for OFDM I and II can be bounded by

$$\begin{aligned} \text{bit rate (bits/subcarrier)} &= E_{\Gamma}[\lg M(\Gamma)] \leq \lg E_{\Gamma}[M(\Gamma)] \quad (6) \\ &= \lg \int_0^{\infty} M(\gamma)g(\gamma)d\gamma \\ &= \lg\left(1 + \frac{1.5}{-\ln 5P_b}\gamma_0\right). \end{aligned}$$

The total bit rate (in the unit of bits/sec) can be easily obtained by scaling with the total number of subcarriers  $N_{FFT}$  and OFDM symbol time  $T_s$  as

$$\text{total bit rate (bits/sec)} \leq \frac{N_{FFT}}{T_s} \lg\left(1 + \frac{1.5}{-\ln 5P_b}\gamma_0\right). \quad (7)$$

The analysis for the bit rate of OFDMA can be done in a similar fashion. Since a subcarrier is assigned to the user with the highest SNR in OFDMA, the subcarrier SNR, denoted  $\Gamma^*$ , is equal to the maximum of  $K$  i.i.d. exponential random variables, where  $K$  is the number of users. The pdf of  $\Gamma^*$  can be derived by a standard algebraic procedure, *i.e.*,

$$g^*(\gamma) = \frac{K}{\gamma_0} \exp\left(-\frac{\gamma}{\gamma_0}\right)(1 - \exp\left(-\frac{\gamma}{\gamma_0}\right))^{K-1}, \quad \gamma \geq 0. \quad (8)$$

Then, by replacing  $\Gamma$  by  $\Gamma^*$  in (6) and following the same derivation procedure, the total bit rate for OFDMA is given by

$$\text{total bit rate (bits/sec)} \leq \frac{N_{FFT}}{T_s} \lg\left(1 + \frac{1.5}{-\ln 5P_b}\gamma_0\left(\sum_{k=1}^K \frac{1}{k}\right)\right). \quad (9)$$

For the BER analysis, it is worthwhile to point out that the bit allocation scheme described in Sec. II guarantees an average BER smaller than the target BER. In other words, all three OFDM modes will achieve comparable average BER if such a bit allocation scheme is employed. To present a more informative comparison in BER, we

may fix the bit rate of three OFDM modes. However, since the actual bit rate determined by the bit allocation scheme is typically different from the target bit rate, we adopt a method similar to [2] to add and subtract bits from proper subcarriers successively until the target bit rate is achieved. This operation will increase (or decrease) the BER when bits are added (or subtracted) as confirmed by simulation in Sec. IV.

### B. Delay-Throughput Analysis

To analyze the queueing delay, a proper queueing model for both OFDM-TDMA and OFDMA is needed for fair comparison. In [8], the M/M/1 model [9] was assumed for users' queues in OFDMA. However, the M/M/1 model may not be suitable in the current context, since the service time of packets, which depends on the actual subcarrier and bit allocation, is not necessarily exponentially distributed. For this reason, a more general queueing model, *i.e.* the M/G/1 model [9], is adopted in our analysis. For the packet arrival process, it is reasonable and fair to assume that it is Poisson distributed with the same rate for both OFDM-TDMA and OFDMA. Packet service is governed by the notion of service time, which can reasonably account for both OFDM-TDMA and OFDMA. One of our main tasks is to find the packet service time for both systems.

The above discussion can be quantified mathematically below. The average delay  $\bar{W}$  in the M/G/1 model is given by [9]

$$\bar{W} = \frac{\lambda E[S^2]}{2(1 - \lambda E[S])}, \quad (10)$$

where  $S$  is the packet service time, and  $\lambda$  is the Poisson packet arrival rate. Please note that, when a queue of an infinite size is assumed as done in our work, the throughput is proportional to the  $\lambda$  value. As shown in (10), we only need to determine  $S$  up to the second moment to determine the average delay for both systems.

Since a packet is served by subcarrier allocation in transmission systems, we consider the service time (and thus delay) being measured in the unit of the number of subcarriers. To be more specific,  $S$  is defined to be the number of subcarriers  $N_s$  satisfying

$$S = \left\{ N_s : U \triangleq \sum_{i=1}^{N_s} \mu_i = \alpha \right\},$$

where  $U$  is the number of bits loaded in  $N_s$  subcarriers,  $\mu_i$  is the number of bits loaded to subcarrier  $i$ , which is identically distributed over all  $i$ , and  $\alpha$  is the fixed packet size in the unit of bits. The idea is explained by a typical OFDM transmission system drawn in Fig. 3, where data streams can be grouped in either a parallel or a serial manner. The "time unit" in serial and parallel groupings are samples and subcarriers, respectively. It is seen that with S/P (serial-to-parallel) and P/S (parallel-to-serial) converters, the conventional notion of delay in the serial grouping translates to the equivalent delay measured in the number of subcarriers in the parallel grouping, and vice versa. This fits into the scheme of OFDM-TDMA as well as OFDMA since we are concerned with the average delay over all users and packets in this work.

We would like to determine the first two moments of  $S$  when

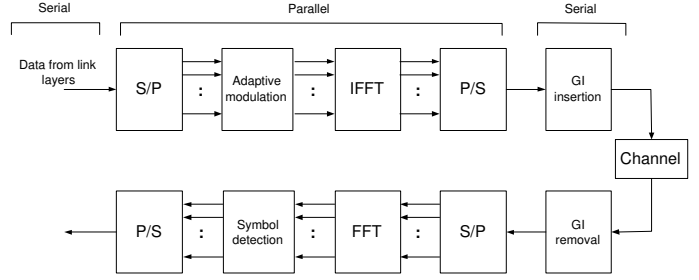


Fig. 3. A typical OFDM transmission system.

$U = \alpha$ . For the first moment, we have

$$\begin{aligned} \alpha &= E[U|U = \alpha] \\ &= E\left[\sum_{i=1}^S \mu_i \mid U = \alpha\right] \\ &= E\left[E\left[\sum_{i=1}^S \mu_i \mid S, U = \alpha\right] \mid U = \alpha\right] \\ &= E\left[SE[\mu_i|U = \alpha] \mid U = \alpha\right] \\ &= E[\mu_i|U = \alpha]E[S|U = \alpha]. \end{aligned}$$

By proper rearrangement, we are led to

$$E[S|U = \alpha] = \frac{\alpha}{E[\mu_i|U = \alpha]}. \quad (11)$$

The second moment can be derived using a similar approach. That is,

$$\begin{aligned} \alpha^2 &= E[U^2|U = \alpha] \\ &= E\left[\left(\sum_{i=1}^S \mu_i\right)^2 \mid U = \alpha\right] \\ &= E\left[E\left[\left(\sum_{i=1}^S \mu_i\right)^2 \mid S, U = \alpha\right] \mid U = \alpha\right] \\ &= E\left[SE[\mu_i^2|U = \alpha] + \sum_{i \neq j} E[\mu_i \mu_j|U = \alpha] \mid U = \alpha\right]. \end{aligned} \quad (12)$$

The cross-term in (12) represents the cross-correlation among subcarriers, which depends on the coherence bandwidth of the channel. Without any further knowledge about the channel, we may proceed in deriving a lower bound. By the Schwartz inequality and the fact that  $\mu_i$  and  $\mu_j$  are nonnegative, we have

$$E[\mu_i \mu_j] \leq \sqrt{E[\mu_i^2]E[\mu_j^2]} = E[\mu_i^2],$$

and consequently,

$$\sum_{i \neq j} E[\mu_i \mu_j|U = \alpha] \leq S(S-1)E[\mu_i^2|U = \alpha]. \quad (13)$$

By plugging (13) into (12) and rearranging the terms, we obtain the following lower bound:

$$E[S^2|U = \alpha] \geq \frac{\alpha^2}{E[\mu_i^2|U = \alpha]}. \quad (14)$$

To complete the analysis in (11) and (14), we need to obtain the first two moments of  $\mu_i$ . Please note that the channel state in the link layer is often modeled by a finite-state Markov chain.

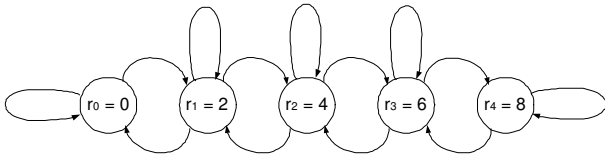


Fig. 4. A finite-state Markov chain model for the channel.

Usually, a channel state corresponds to a certain channel condition and/or a certain modulation scheme. As shown in Fig. 4, the five states correspond to five M-QAM modulations, where  $r_i$  indicates the number of bits employed in the modulation. The transition probability, which was derived before (*e.g.*, [5]), is not of our concern here. Our interest is to calculate the steady-state probabilities  $\pi_i$ 's. They can be obtained by integrating pdf in (5) and (8) over each region illustrated in Fig. 2. Thus, we have

$$\pi_i = \int_{b_i}^{b_{i+1}} g(\gamma) d\gamma \text{ for OFDM I \& II,} \quad (15)$$

and

$$\pi_i = \int_{b_i}^{b_{i+1}} g^*(\gamma) d\gamma \text{ for OFDMA,} \quad (16)$$

where  $i = 0, 1, 2, 3, 4$ . With these calculated  $\pi_i$ 's, the first and second moments of  $\mu_i$  can be easily obtained by

$$E[\mu_i | U = \alpha] = \sum_{i=0}^4 \pi_i \cdot r_i, \quad (17)$$

$$E[\mu_i^2 | U = \alpha] = \sum_{i=0}^4 \pi_i \cdot r_i^2. \quad (18)$$

Note that the condition on  $U = \alpha$  does not change the moments  $\mu_i$ .

Finally, by plugging (17) and (18) in (11) and (14), and then (11) and (14) in (10), we obtain the theoretical throughput-delay lower bound curves. Note that, as the throughput value approaches capacity ( $\lambda \rightarrow 1/E[S]$ ), the average delay goes up to infinity. This result will be verified by computer simulation in the next section.

#### IV. SIMULATION RESULTS

We perform computer simulation to verify the analysis given in Sec. III and make an extensive comparison of the link and the physical layer performance of OFDM-TDMA and OFDMA in this section.

The Rayleigh fading channel is adopted in the simulation. It is generated by a tapped delay line (TDL) channel model with equally-spaced taps and an exponential power delay profile. The parameters chosen for the TDL channel model are given in Table II. We consider a total of  $K = 4$  users, whose channel coefficients are i.i.d. A fast fading channel based on the method described in [10] is implemented. That is, the channel varies, presumably independently, across OFDM frames while remains the same within a frame. Although OFDMA typically has a larger number of subcarriers than OFDM in real world applications, we use an identical set of parameters for both systems for fair comparison. The parameters of the OFDM system are borrowed from [11] and summarized in Table III.

We first examine the total bit rate that can be supported by each mode. The analytical results from (7) and (9) and empirical results are shown in Fig. 5. Note that a target BER of  $10^{-3}$  is set for bit allocation, and a frame size equal to ten OFDM symbols is adopted. We see that, for a given SNR level, OFDMA outperforms OFDM II while OFDM II outperforms OFDM I. The difference between

TABLE II  
THE TDL CHANNEL MODEL PARAMETERS

rms delay spread ( $\tau_{rms}$ )	1 $\mu$ s
tap spacing ( $T$ )	175 ns
number of taps ( $L$ )	20
max delay spread ( $\tau_{max}$ )	3.325 $\mu$ s (= 175 ns $\times$ (20-1))

TABLE III  
PARAMETERS OF THE OFDM SYSTEM

OFDM symbol time ( $T_s$ )	100.8 $\mu$ s
useful symbol time ( $T_b$ )	89.6 $\mu$ s
guard time ( $T_g$ )	11.2 $\mu$ s
FFT size ( $N_{FFT}$ )	512
sample time ( $T$ )	175 ns (= 89.6 $\mu$ s/512)

OFDM I and OFDM II comes from dynamic allocation, which is also known as the multiuser diversity gain. OFDMA achieves the best bit rate performance, since there is an additional frequency diversity for OFDMA as compared with OFDM II. Since we consider modulation up to 256-QAM in the simulation, all three curves will approach the same bit rate as SNR increases.

Fig. 6 shows the uncoded BER performance when the bit rate is fixed at 4 bits/subcarrier, or  $2 \times 10^7$  bits/sec. We see that the BER is above the target BER (=  $10^{-3}$ ) at the low SNR region. This is because the bit allocation scheme actually selects a bit rate lower than 4 bits/subcarrier in this region. However, extra bits are added to make up 4 bits/subcarrier, thus increasing the BER above the target one. Also, we see from Fig. 6 that OFDMA outperforms OFDM II by 3.5 dB and OFDM II outperforms OFDM I by 2 dB when BER =  $10^{-3}$ .

The throughput-delay performance curves at the packet level are shown in Fig. 7. The packet size  $\alpha$  is chosen to be 80 bits as used in speech applications [12], and a frame size of one OFDM symbol is adopted here. In the simulation as shown in Fig. 8, we consider an exhaustive service system where only packets that arrived before or during the current frame can be served in the current frame. This is a more realistic assumption. Besides, the number of packets in a queue is counted on a frame-by-frame basis, and these numbers are averaged to give a finite granularity approximation of  $\bar{N}$ , which is

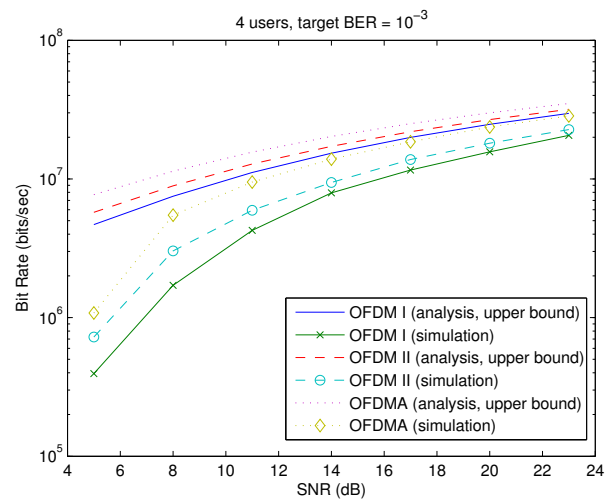


Fig. 5. Comparison of the maximum bit rates that can be supported by the three modes.

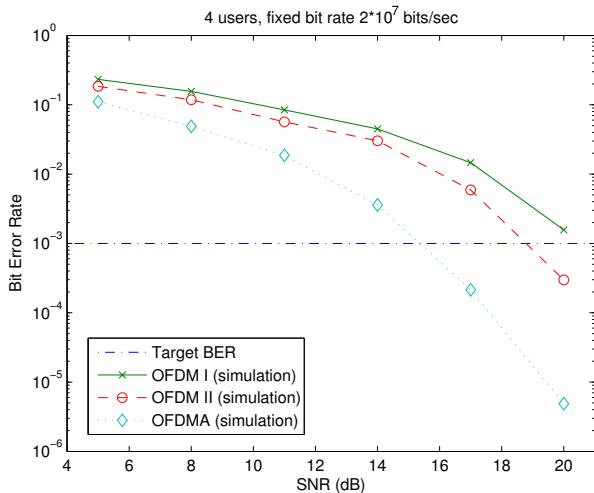


Fig. 6. Comparison of BER results for three modes.

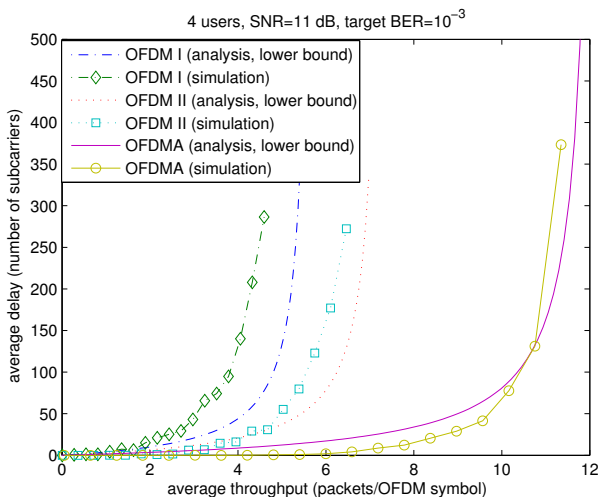


Fig. 7. Comparison of the packet throughput and delay results.

the average number of packets in the queue. With  $\bar{N}$  and throughput  $\lambda$  controlled to get different points on the plot, we can calculate the average delay  $\bar{W}$  by Little's Theorem [9]:

$$\bar{W} = \frac{\bar{N}}{\lambda}. \quad (19)$$

Note that there is no notion of “frame” in the analytical M/G/1 model. In other words, seamless service is assumed. However, in the finite granularity implementation, a frame should be considered. This accounts for the fact that the simulation curve does not obey the analytical lower bound curve when the throughput is low. In fact, due to the exhaustive service assumption and frame-by-frame approximation of  $\bar{N}$ , the value of  $\bar{N}$  tends to be close to zero when the throughput is low, resulting a value of  $\bar{W} \approx 0$ . We see from Fig. 7 that, given a fixed delay, OFDMA has the largest throughput (measured in packets/OFDM symbol), OFDM II the second, and OFDM I the third.

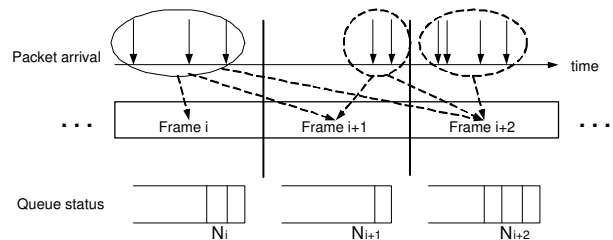


Fig. 8. Illustration of the exhaustive service system and queuing in the link layer simulation.

## V. CONCLUSION AND FUTURE WORK

Performance comparison of OFDM-TDMA and OFDMA centered on scheduling with cross-layer consideration was conducted in this work. Several subcarrier assignment and bit allocation methods were implemented to obtain three OFDM modes. We provided an analytical framework for performance analysis. Furthermore, the performance was compared in terms of bit rate, BER, packet throughput and delay so that we have a thorough understanding of the system from the viewpoint of both link and physical layers. From the analysis and simulation results, we concluded that dynamic OFDMA outperforms dynamic OFDM-TDMA in achieving a lower BER and a higher throughput under the same delay requirement. Our future work includes the comparison in an environment where there exists heterogeneous traffic among different users.

## REFERENCES

- [1] C. Eklund, R. B. Marks, K. L. Stanwood, and S. Wang, “IEEE standard 802.16: A technical overview of the WirelessMAN air interface for broadband wireless access,” *IEEE Commun. Mag.*, vol. 40, pp. 98–107, June 2002.
- [2] A. Czylik, “Adaptive OFDM for wideband radio channels,” in *Proc. IEEE Global Telecommunications Conf. (GLOBECOM'96)*, Nov. 1996, pp. 713–718.
- [3] H. Rohling and R. Grunheid, “Performance comparison of different multiple access schemes for the downlink of an OFDM communication system,” in *Proc. IEEE Vehicular Technology Conf. (VTC'97)*, May 1997, pp. 1365–1369.
- [4] C. Y. Wong, R. S. Cheng, K. B. Letaief, and R. D. Murch, “Multiuser OFDM with adaptive subcarrier, bit, and power allocation,” *IEEE J. Select. Areas Commun.*, vol. 17, pp. 1747–1758, Oct. 1999.
- [5] Q. Zhang and S. A. Kassam, “Finite-state Markov model for Rayleigh fading channels,” *IEEE Trans. Commun.*, vol. 47, pp. 1688–1692, Nov. 1999.
- [6] D. Tse and P. Viswanath, *Fundamentals of Wireless Communication*. Cambridge University Press, 2005.
- [7] M. Alouini and A. J. Goldsmith, “Adaptive modulation over Nakagami fading channels,” *Wireless Personal Communications*, vol. 13, pp. 119–143, May 2000.
- [8] G. Song, Y. Li, J. Leonard J. Cimini, and H. Zheng, “Joint channel-aware and queue-aware data scheduling in multiple shared wireless channels,” in *Proc. IEEE Wireless Communications and Networking Conf. (WCNC'04)*, 2004, pp. 1939–1944.
- [9] D. Bertsekas and R. Gallager, *Data Networks*, 2nd ed. Prentice Hall, 1991.
- [10] P. Viswanath, D. N. C. Tse, and R. Laroia, “Opportunistic beamforming using dumb antennas,” *IEEE Trans. Inform. Theory*, vol. 48, pp. 1277–1294, June 2002.
- [11] H. Yaghoobi, “Scalable OFDMA physical layer in IEEE 802.16 WirelessMAN,” *Intel Technology Journal*, vol. 8, pp. 201–212, Aug. 2004.
- [12] J. C. De Martin, “Source-driven packet marking for speech transmission over differentiated-services networks,” in *Proc. IEEE Int. Conf. Acoustics, Speech, and Signal Processing (ICASSP'01)*, 2001, pp. 753–756.